

## EULER BUCKLING

By E.C. Zeeman

Mathematics Institute, University of Warwick.

There has recently been a fruitful interaction between elasticity theory and catastrophe theory. This paper offers an introduction, by giving an elementary exposition of the classical buckling beam in terms of cusp catastrophes. The last section on globalisation contains new material. See also [1,2,4,8]. Many other interesting examples can be found in the book [6] of Michael Thompson and Giles Hunt.

The study of instability of structures leads naturally to the analysis of the first few terms of Taylor expansions of energy functions of several variables, in order to find the equilibria. Thus several authors, including W.T. Koiter [11] as early as 1945, and in the 1960's M.J. Sewell [12], Thompson and Hunt, had independently discovered some of the elementary catastrophes. Note particularly Hunt's elegant computer drawings of the elliptic and hyperbolic umbilics [7,8], made before he had heard of Thom's classification theorem. However these discoveries were computations of particular approximations, rather than the recognition that the elementary catastrophes were diffeomorphism invariants. What catastrophe theory has to offer to elasticity theory is theorems, proofs, and higher dimensional singularities for handling compound buckling. Meanwhile, in return, what elasticity theory has to offer to catastrophe theory is an abundance of examples, fresh insights and problems. I am indebted to David Chillingworth, Maurice Dodson, Tim Poston and Michael Thompson for discussions.

### Contents.

1. The simple Euler arch.
2. The Euler strut.
3. The pinned Euler strut.
4. Globalisation.

## 1. THE SIMPLE EULER ARCH.

We begin with a simple example consisting two rigid arms supported at the ends and pivoted together at the centre, with a spring tending to keep them at  $180^\circ$ , as illustrated in Figure 1.

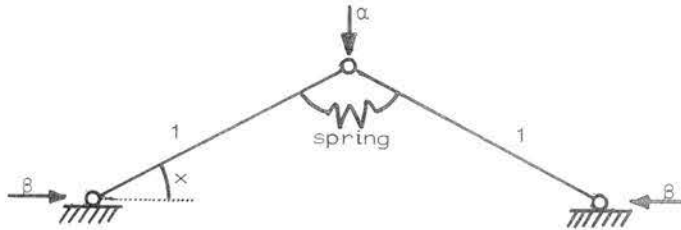


Figure 1. The simple Euler arch.

If the ends are compressed with a gradually increasing horizontal force  $\beta$  then the arms will remain horizontal until  $\beta$  reaches a critical value, when they will begin to buckle upwards (or downwards). If  $\beta$  is now fixed, and a gradually increasing vertical load  $\alpha$  is applied to the pivot, as in Figure 1, then the arch will support the load until  $\alpha$  reaches a critical value, when it will suddenly snap catastrophically into the downwards position. It is this behaviour that we shall explain by our first cusp catastrophe.

Suppose that the arms each have length 1, and let  $\mu$  denote the modulus of elasticity of the spring. Initially we assume  $\alpha = 0$ .

Theorem 1. The arch buckles when  $\beta = 2\mu$ .

Before proving theorem 1, we go on to describe what happens in the neighbourhood of the buckling point. Let  $\beta = 2\mu + b$ , and let  $x$  denote the angle of the arms to the horizontal. We assume  $\alpha, b, x$  are small. In 3-dimensions choose the  $(\alpha, \beta)$ -axes horizontal, and the  $x$ -axis vertical. Call the horizontal  $(\alpha, \beta)$ -plane the control plane,  $C$ . Let  $M$  be the graph of  $x$  as a function of  $\alpha, \beta$ .

Theorem 2.  $M$  is a cusp catastrophe with  $(-\alpha)$  as normal factor and  $\beta$  as splitting factor (Figure 2).

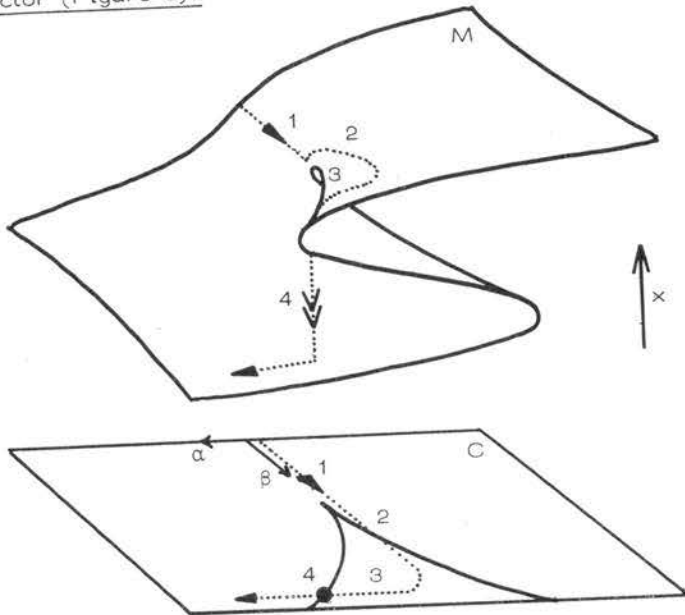


Figure 2. The dotted path shows the arch (1) compressed, (2) buckling upwards, (3) loaded, and (4) snapping downwards.

Proof of Theorem 1.

$$\text{Energy in spring} = \frac{1}{2} \mu (2x)^2.$$

$$\text{Energy gained by load} = \alpha \sin x.$$

$$\text{Energy lost by compression} = -2\beta(1 - \cos x)$$

$$\therefore \text{total energy, } V = 2\mu x^2 + \alpha \sin x - 2\beta(1 - \cos x).$$

The surface  $M$  of equilibria is given by  $V' = 0$ , where the prime denotes  $\partial/\partial x$ .

The fold lines are given by  $V'' = 0$ , and the cusp point by  $V''' = 0$ .

$$V' = 4\mu x + \alpha \cos x - 2\beta \sin x = 0$$

$$V'' = 4\mu - \alpha \sin x - 2\beta \cos x = 0$$

$$V''' = -\alpha \cos x + 2\beta \sin x = 0.$$

Add the first and last :  $4\mu x = 0$ . But  $\mu \neq 0$ .  $\therefore x = 0$ .

Substitute in the first :  $\alpha \cos x = 0$ .  $\therefore \alpha = 0$ .

Substitute in the second :  $4\mu - 2\beta = 0$ .  $\therefore \beta = 2\mu$ .

This completes the proof of Theorem 1.

Proof of Theorem 2. Put  $\beta = 2\mu + b$ . Let  $O^5$  denote  $O(x^5)$ . Therefore

$$\begin{aligned} V &= 2\mu x^2 + \alpha \left(x - \frac{x^3}{6}\right) + 2(2\mu + b) \left(-\frac{x^2}{2} + \frac{x^4}{24}\right) + O^5 \\ &= \alpha x - bx^2 - \frac{\alpha}{6}x^3 + \frac{2\mu + b}{12}x^4 + O^5. \end{aligned}$$

$$\text{When } \alpha = b = 0, V = \frac{\mu}{6}x^4 + O^5.$$

Hence  $x$  obeys a cusp catastrophe since  $\mu > 0$ . We can eliminate the  $x^3$ -term by the translation of coordinates  $x = x_1 + \frac{\alpha}{2(2\mu + b)}$ , and then eliminate the tail of the Taylor series by a non-linear change of coordinates by [9, Theorem 2.9]

Therefore

$$V \sim \frac{\mu}{6}x^4 + \alpha x - bx^2,$$

by the isomorphism of unfoldings [9, Theorem 6.9]. This is the potential for a cusp catastrophe with  $(-\alpha)$  as normal factor and  $b$  (or  $\beta$ ) as splitting factor, thus completing the proof of Theorem 2 and Figure 2.

## 2. THE EULER STRUT.

We now turn from the discrete to the continuous, from the simple pivot to the elastic strut\*, compressed under force  $\beta$ , as shown in Figure 3.

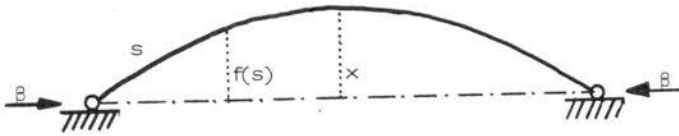


Figure 3. The Euler strut.

Let  $\lambda$  denote the length of the strut, and  $\mu$  the modulus of elasticity per unit length.

Theorem 3 (Euler [3] 1744). The strut buckles when  $\beta = \mu(\pi/\lambda)^2$ . The buckled shape is a sine-curve, to second order.

Proof. Let  $s$  be a parameter for arc-length,  $0 \leq s \leq \lambda$ . Let  $f(s)$  denote the vertical displacement of the point  $s$ , which we assume is small. The shape of the strut is therefore given by the function  $f: [0, \lambda] \rightarrow \mathbb{R}$ . We assume  $f$  is a  $C^\infty$ -function satisfying the boundary conditions :

$$f = 0 \text{ at the ends (since the ends are supported),}$$

$$f'' = 0 \text{ at the ends (since there is no bending moment there),}$$

where primes denote  $\partial/\partial s$ . Let  $\theta(s)$  be the inclination of the strut to the horizontal at  $s$ . Then

---

\* The Battelle Research Centre conveniently provides plastic Euler struts for stirring coffee, which when held between thumb and forefinger make excellent experimental material; otherwise try using a 1" x 4" piece of thin cardboard. See Figure 7.

$$f' = \sin \theta$$

$$f'' = \cos \theta \cdot \theta'$$

$$\begin{aligned} \therefore \text{curvature} = \theta' &= \frac{f''}{\cos \theta} \\ &= f''', \text{ neglecting fourth order terms.} \end{aligned}$$

$$\therefore \text{energy in increment } ds \text{ of strut} = \frac{1}{2}(\mu ds)(f''')^2$$

$$\therefore \text{energy in strut} = \frac{1}{2} \int_0^\lambda \mu (f''')^2 ds$$

$$\begin{aligned} \text{The contraction between the ends} &= \int_0^\lambda (1 - \cos \theta) ds \\ &= \frac{1}{2} \int (f')^2 ds \end{aligned}$$

$$\therefore \text{energy lost by compression force} = -\frac{1}{2} \int \beta (f')^2 ds$$

$$\therefore \text{total energy, } V = \int F ds, \text{ where } F = \frac{1}{2}[\mu (f''')^2 - \beta (f')^2].$$

By the calculus of variations, using the boundary condition, the requirement for equilibrium is given by the Euler equation

$$\left( \frac{\partial F}{\partial f'''} \right)'' - \left( \frac{\partial F}{\partial f'} \right)' = 0$$

$$\therefore \mu f'''' + \beta f' = 0.$$

Solving this equation, using the boundary conditions,

$$f(s) = x \sin(s/\sqrt{\beta/\mu}),$$

where  $x = \text{constant}$ , and  $\lambda\sqrt{\beta/\mu}$  is a multiple of  $\pi$ . Therefore, if  $\beta < \mu(\pi/\lambda)^2$ , only the zero solution is possible. Buckling first begins when

$\beta = \mu(\pi/\lambda)^2$  and then, to second order,

$$f(s) = x \sin \frac{\pi s}{\lambda}, \quad x \text{ small constant.}$$

The solution is correct to second order because the next term is of order  $x^3$  (see below). This completes the proof of Theorem 3.

### Harmonics.

Write  $f$  as the Fourier series  $f(s) = \sum_1^\infty x_n \sin \frac{n\pi s}{\lambda}$ . We call  $x_n$  the  $n^{\text{th}}$  harmonic of  $f$ .

Meaning of  $x$ .

The constant  $x$  occurring in the proof of Theorem 3 above can be interpreted in three ways, which agree to first order, but differ in higher orders :

- (i)  $x$  is the vertical displacement of the centre of the strut.
- (ii)  $x$  is the first harmonic of  $f$ .
- (iii)  $x$  is a perturbation parameter.

Using  $x$  in the last sense, one can expand  $f$  by perturbation theory; see for example [6, pages 28-34] :

$$f = x - \frac{1}{64} (\pi/\lambda)^2 [\sin(\pi s/\lambda + (3\pi s/\lambda))] x^3 + O^5$$

$$\beta = \mu(\pi/\lambda)^2 + \frac{1}{4} \mu(\pi/\lambda)^4 x^2 + O^4$$

Qualitative approach.

The disadvantage of perturbation theory is that it tends to carry us away from the conceptual point of view of regarding the compression force  $\beta$  as the "cause" and the shape  $f$  as the "effect". What we really want to do is to use the perturbation expansion to draw the graph  $G$  of  $f$  as a function of  $\beta$ , as in Figure 4. (Alternatively we could use Theorem 5 below to deduce the shape of  $G$ .)

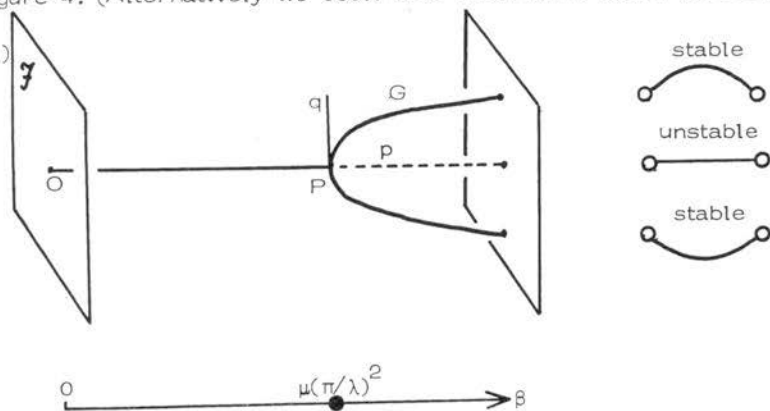


Figure 4. The graph  $G$  of shape  $f$  as a function of compression  $\beta$ .

The graph is stably constant  $f = 0$  up to the Euler buckling force, where it bifurcates parabolically at the point  $P$  into two stable branches, representing buckling upwards and downwards, while  $f = 0$  becomes an unstable branch.

There are two technical difficulties about this graph: firstly  $G$  has a singularity at  $P$ , and secondly the space  $\mathcal{F}$  in which  $f$  lies (which we have drawn as 2-dimensional in Figure 4) is in fact  $\infty$ -dimensional. Catastrophe theory helps us to get rid of the first difficulty as follows. Observe that  $G$  is equivalent to the section  $\alpha = 0$  of the surface in Figure 2. Therefore if we introduce a small vertical load  $\alpha$  on the centre of the strut, then the  $\beta$ -axis will be embedded in a 2-dimensional control plane  $C$ , with coordinates  $(\alpha, \beta)$ , and  $G$  will be embedded in a smooth equilibrium surface  $M \subset C \times \mathcal{F}$ , such that the projection  $M \rightarrow C$  is a cusp catastrophe.

Meanwhile the second difficulty of  $\infty$ -dimensionality can be either met or avoided; Chillingworth [1] shows how to meet it by embedding  $\mathcal{F}$  in a Hilbert space, but here we shall avoid it, as follows. We capture the qualitative behaviour by selecting the significant harmonic, which in this case is the first harmonic, and computing it to first order. To study the quantitative behaviour one could equally well compute a finite number of harmonics up to the required accuracy. More precisely, let  $h: \mathcal{F} \rightarrow \mathbb{R}$  be the function mapping  $f$  to its first harmonic,  $h(f) = x$ . Then, although  $1 \times h: C \times \mathcal{F} \rightarrow C \times \mathbb{R}$  crushes  $(2+\infty)$ -dimensions down onto 3-dimensions, it nevertheless does not crush the equilibrium surface  $M$  that interests us, but embeds  $M$  smoothly into  $C \times \mathbb{R}$ , enabling us to visualise it and compute it.

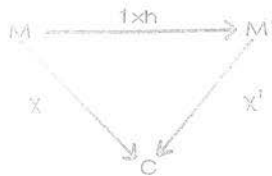
Lemma 4.  $1 \times h$  maps a neighbourhood of  $P$  in  $M$  diffeomorphically into  $C \times \mathbb{R}$ .

Proof. Let  $p, q$  denote the two tangent lines to  $G$  at  $P$ . In Figure 3  $p$



coincides with the line  $f = 0$ , and is horizontal parallel to the  $\beta$ -axis, while  $q$  is tangent to the parabola, and vertical in the sense of being parallel to  $\mathcal{F}$ . By the proof of Theorem 3 the derivative  $Dh$  maps  $q$  isomorphically onto  $R$ , and hence  $D(1xh)$  maps the plane spanned by  $\{p, q\}$  isomorphically into  $C \times R$ . But this is the tangent plane to  $M$  at  $P$ . Therefore  $1xh$  maps a neighbourhood of  $P$  in  $M$  diffeomorphically into  $C \times R$ .

Let  $M' = (1xh)M$ ,  $P' = (1xh)P$ . Then we have a commutative diagram



where  $\chi, \chi'$  are induced by projection.

Corollary. The singularity of  $\chi$  at  $P$  is equivalent to that of  $\chi'$  at  $P'$ .

Therefore to prove that  $M$  is a cusp catastrophe it suffices to show that  $M'$  is. Thus we have avoided the  $\infty$ -dimensional problem, because we work with  $M' \subset C \times R$ , which is 3-dimensional.

For convenience choose units so that the length of the strut,  $\lambda = \pi$ , and the modulus of elasticity per unit length,  $\mu = 1/\pi$ . Then the Euler buckling force  $= \mu = 1/\pi$ . Let  $\beta = (1+b)/\pi$ , and assume  $x, a, b$  are small.

Theorem 5.  $M'$  is a cusp catastrophe with  $(-a)$  as normal factor and  $\beta$  as splitting factor. In other words the Euler strut behaves exactly as the simple Euler arch in Theorem 2 and Figure 2.

Proof. By Theorem 3,  $f = x \sin s + O^3$ .

$$\begin{aligned} \therefore \text{energy in strut} &= \frac{1}{2} \int_0^\pi \mu (f'')^2 (1 - (f')^2)^{-1} ds, \\ &= \frac{1}{2\pi} \int x^2 \sin^2 s (1 + x^2 \cos^2 s) ds + O^6 \\ &= \frac{1}{4}(x^2 + \frac{1}{4}x^4) + O^6, \end{aligned}$$

because the other  $O^4$ -terms disappear in the integration.

$$\begin{aligned} \text{Energy lost by compression} &= -\int \beta [1 - \sqrt{1 - (f')^2}] ds \\ &= -\frac{\beta}{2} \int (x^2 \cos^2 s + \frac{1}{4}x^4 \cos^4 s) ds + O^6 \\ &= -\frac{1}{4}(1+b)x^2 + \frac{3x^4}{16} + O^6. \end{aligned}$$

$$\text{Energy gained by load} = \alpha(x + O^3)$$

$$\begin{aligned} \therefore \text{total energy, } V &= \frac{1}{64}x^4 + \alpha(x + O^3) - b(\frac{1}{4}x^2 + O^4) + O^6 \\ &\sim \frac{1}{64}x^4 + \alpha x - \frac{1}{4}bx^2. \end{aligned}$$

This completes the proof of Theorem 4.

## 3. THE PINNED EULER STRUT

We now turn to a much more interesting property of the Euler strut, namely its load bearing capacity and imperfection sensitivity, when the ends are pinned as in Figure 5.

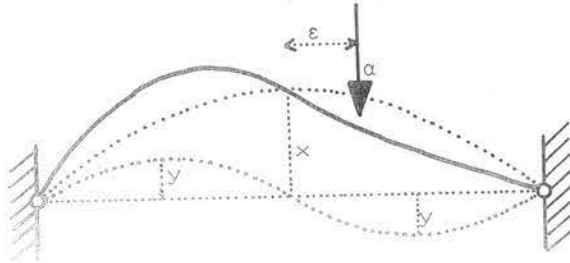


Figure 5. In the pinned Euler strut with an offset load the second harmonic  $y$  is significant.

Let  $r$  be the first harmonic when the strut is unloaded;  $r$  is a constant related to the difference between the length of the strut and the distance between the pins. We now apply a vertical load  $\alpha$  off-set from the centre by a distance  $\epsilon$ , as shown in Figure 5. We call  $\epsilon$  the imperfection, because this model sometimes simulates a manufacturing imperfection. The question is: when will the strut snap catastrophically into the downwards position? This time the second harmonic will be the significant one, as shown in Figure 5.

A nice realisation in stone of Figure 5 can be seen in the western arch of Clare College bridge over the river Cam, in which the keystone is about  $10^\circ$  to the vertical.

Theorem 3. The graph of  $y$  as a function of  $(\alpha, \epsilon)$  is a dual cusp catastrophe, with  $\epsilon$  as normal factor and  $(-\alpha)$  as splitting factor.

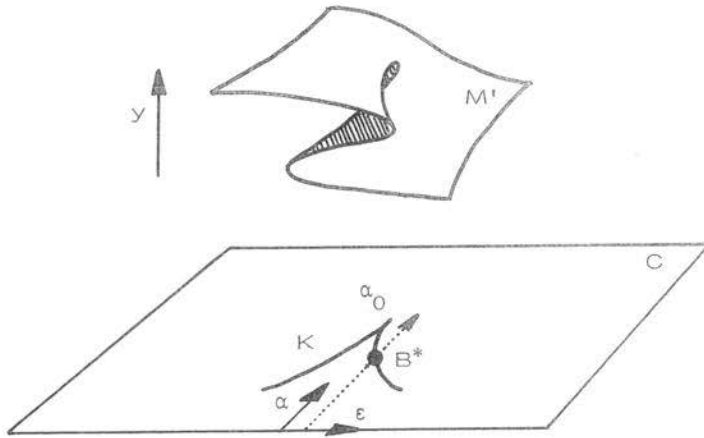


Figure 6. In the pinned Euler strut the second harmonic  $y$  obeys a dual cusp catastrophe. The cusp  $K$  illustrates the load carrying capacity and imperfection sensitivity.

Remark 1. Here the word dual means that the middle sheet represents stable equilibria, while the upper and lower sheets represent unstable equilibria. We call  $\varepsilon$  the normal factor, rather than  $(-\varepsilon)$ , because on the stable middle sheet  $y$  increases with  $\varepsilon$ .

Remark 2. Theorem 6 is a local statement and therefore we have only drawn the graph over a neighbourhood of the cusp point. In particular the result does not extend to  $\alpha = 0$ . We shall treat  $\alpha = 0$  in the globalisation below.

Load carrying capacity. The cusp  $K$  in Figure 6 is the bifurcation set. If the load  $\alpha$  is gradually increased keeping the imperfection

$\varepsilon$  fixed, as shown on the dotted path, then the stability of the upward position of the strut breaks down when the path crosses K at the point  $B^*$ , and the strut will snap catastrophically into the downward position. The latter is represented by another sheet of stable equilibria, which is not shown in Figure 6, but is explained in Figure 8 and Theorem 9 below.

The cusp K is therefore the graph in C of the load carrying capacity  $\alpha$  as a function of the imperfection  $\varepsilon$ . The sharp reduction in load carrying capacity away from the maximum  $\alpha_0$  by the  $\frac{2}{3}$ -power law of the cusp is called imperfection-sensitivity. Obviously this can be critical in designing structures. Ronalds [3, 3 Figure 44] has tested struts of high-tensile steel, and obtained accurate experimental confirmation of the cusp. Before proving Theorem 5 we compute the maximum load.

Lemma 7. The first harmonic  $x$  and the second harmonic  $y$  are related by the equation  $x^2 + 4y^2 = r^2$ .

Proof. As before suppose  $\lambda = \pi$ ,  $\mu = 1/\pi$ . We shall work to  $O^2$ , and ignore higher harmonics. Therefore

$$f = x \sin s + y \sin 2s.$$

$$\begin{aligned} \text{Distance between pins} &= \int_0^\pi \sqrt{1 - (f')^2} ds \\ &= \int_0^\pi (1 - \frac{1}{4}(x \cos s + 2y \cos 2s)^2) ds \\ &= \pi(1 - \frac{1}{4}x^2 - y^2) \\ &= \pi(1 - \frac{3}{4}r^2) \quad \text{when the strut is unloaded.} \\ \therefore x^2 + 4y^2 &= r^2. \end{aligned}$$

Lemma 8. The maximum load is  $\alpha_0 = \frac{3r}{2}$ .

Proof. Energy in strut =  $\frac{1}{2} \int \mu (f'')^2 ds$   
 $= \frac{1}{4} (x^2 + 16y^2)$   
 $= \frac{1}{4} (r^2 + 12y^2)$ , by Lemma 7.

Energy of load =  $\alpha f(\pi/2 + \varepsilon)$   
 $= \alpha(x - 2\varepsilon y)$ , ignoring  $\varepsilon^2$   
 $= \alpha(r - \frac{2y^2}{r} - 2\varepsilon y)$ , by Lemma 7.

$\therefore$  total energy,  $V = \text{constant} - 2\alpha\varepsilon y + (3 - \frac{2\alpha}{r})y^2$ .

The cusp point occurs when  $V' = V'' = 0$ , where prime denotes  $\partial/\partial y$ .

Therefore  $\varepsilon = 0$  and  $\alpha = \frac{3r}{2}$ .

Proof of Theorem 6. We can either work locally with higher orders or globally with order 2, and since both approaches shed light we shall do both. First we work locally, and show that  $y$  satisfies a dual cusp catastrophe by computing the coefficient of  $y^4$  in the expansion of  $V$ , and verifying that it is negative. Since we are working near the cusp point we may assume  $y \ll r$ . Therefore we shall suppose  $r, x = O^1$ ,  $y = O^2$ , and ignore higher harmonics. Then working to order  $O^6$  gives a refinement of Lemma 7 :

$$x^2 + 4y^2 + \frac{3}{2}x^2y^2 = r^2$$

$$\therefore x = r - \frac{2y^2}{r} - \frac{3ry^2}{4} - \frac{2y^4}{r^3}$$

Energy in strut = constant +  $(3 + \frac{13r^2}{8})y^2$

Energy in load =  $\alpha(x - 2\varepsilon y)$ , ignoring  $\varepsilon^2$   
 $= \alpha[r - 2\varepsilon y - (\frac{2}{r} + \frac{3r}{4})y^2 - \frac{2y^4}{r^3}]$

$\therefore$  total energy = const -  $2\alpha\varepsilon y + [(3 + \frac{13r^2}{8}) - \alpha(\frac{2}{r} + \frac{3r}{4})]y^2 - \frac{2\alpha y^4}{r^3}$ .

$\therefore \alpha_0 = \frac{3r}{2} - \frac{r^3}{4}$ .

Put  $\alpha = \alpha_0 + a$ .

$\therefore V \sim \frac{3}{r^2}y^4 - 3r\varepsilon y - \frac{2}{r}ay^2$   
 $\sim -(y^4 + \varepsilon y + ay^2)$ , absorbing the constants in the

variables. This is the potential of a dual cusp with normal factor  $\epsilon$  and splitting factor  $(-a)$ , completing the proof of Theorem 6.

#### A simple constraint experiment.

We can obtain the shape of Figure 5 by holding a plastic or cardboard strut between thumb and forefinger as shown in Figure 7(a), and constraining it by pushing slowly down, off centre.

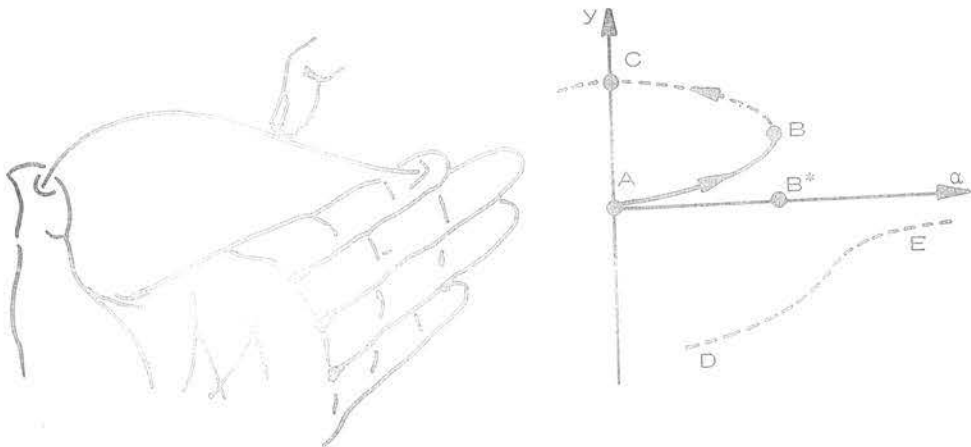


Figure 7. (a) Experiment with a plastic or cardboard strut, and (b) the resulting graph of load  $\alpha$  and second harmonic  $y$ .

However this experiment is slightly different from that described by Theorem 6 because the push down is a constraint rather than a load. It is true that the constraint will exert a downward load equal to the upward resistance of the strut, which is exactly what is needed to keep it in equilibrium, but the nature of the stability changes: for example an equilibrium point on the upper sheet of Figure 6, which would be unstable with respect to a fixed load, becomes stable with respect to a fixed constraint. We can test this as follows.

Figure 7(b) shows the section of Figure 6 over the dotted path through  $B^*$ , extended back to  $\alpha = 0$ . The black curve AB is the section of the stable middle sheet, and the dotted curves BC, DE are the sections of the unstable upper and lower sheets. The point A represents the initial unloaded shape with maximum first harmonic and zero second harmonic. As the strut is slowly pushed down it follows smoothly the curve AB; a steadily increasing load is required, and the second harmonic grows noticeably. B is the fold point over  $B^*$ , and would be the point where strut would have snapped into the downward position in the loading experiment of Theorem 6. But here we are constraining rather than loading, and the constraint does not continue to exert the critical load  $B^*$ ; instead the actual load applied by the constraint begins to decrease again, and the behaviour, instead of snapping, continues to follow smoothly round the curve BC. The change in the nature of the stability can be detected by observing that for points on AB a push down increases the resistance of the strut, whereas for points on BC a push down decreases the resistance. Eventually the point C is reached, which represents maximum second harmonic and zero first harmonic; here the resistance changes sign, and so the constraint no longer constrains, allowing the strut at last to snap into the downward position.



## 4. GLOBALISATION

The disadvantage of Theorem 6 is that it only gives a local analysis near the cusp point. Similarly the disadvantage of Figure 6 is that does not show the other sheet of stable equilibria, representing the strut in the downward positions,  $x < 0$ . Although the cusp  $K$  tells us where the catastrophic jumps will occur, and although the fold curves above tell us where they jump from, we cannot see where they will jump to, because this receiving sheet is missing. And indeed, were we to include the missing sheet on Figure 6, this would be even more confusing because it would intersect the other sheets already there.

To clarify matters we must use the first harmonic as well as the second. Let  $H$  be the plane with coordinates  $(x,y)$  representing both harmonics, and let  $h: \mathcal{F} \rightarrow H$  denote the map  $f \mapsto (x,y)$ . We are interested in the equilibrium surface  $M \subset C \times \mathcal{F}$ . The relation  $x^2 + 4y^2 = r^2$  of Lemma 7 determines an ellipse  $E \subset H$ . Therefore the product map

$$1xh: C \times \mathcal{F} \rightarrow C \times H$$

maps  $M$  onto a surface  $M'$  inside the solid torus  $C \times E$ . The questions we want to answer are :

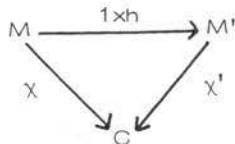
What is the geometry of  $M'$ ?

How does  $M'$  lie in  $C \times E$ ?

What is the singular set of the projection  $\chi': M' \rightarrow C$ ?

What is the bifurcation set,  $\text{Bif } \chi' = \chi'(\text{Sing } \chi')$ ?

If we can show  $M'$  is smooth, then  $1xh$  must have mapped  $M$  diffeomorphically on to  $M'$ , and so the commutative diagram



ensures that  $\text{Bif } \chi = \text{Bif } \chi'$ . Therefore an analysis of  $M'$  will reveal the global catastrophe set,  $\text{Bif } \chi$ , that we are looking for.

### Torque.

The moment of the load  $\alpha$  about the mid-point between the pins is  $\alpha\varepsilon$ . Define the torque  $\tau = \frac{1}{2}\alpha\varepsilon$ . (The factor  $\frac{1}{2}$  is included for technical convenience in the proof of Theorem 9 below.) Locally Theorem 6 and Figure 6 remain the same if the imperfection  $\varepsilon$  is replaced by the torque  $\tau$ , because, for  $\alpha$  bounded away from zero (as it is in Theorem 6), the change of variable  $\varepsilon \rightarrow \tau$  is a diffeomorphism and the cusp catastrophe is invariant under diffeomorphism. Globally  $\tau$  is more convenient than  $\varepsilon$ , and so from now on we use  $\tau$ . Therefore the control plane  $C$  will now have coordinates  $(\alpha, \tau)$ . In particular the control point  $\alpha = 0, \tau \neq 0$  means apply torque, without load, to the centre of the strut.

### Construction.

We make a mysterious construction. Let  $j: H \rightarrow C$  be the linear isomorphism given by

$$\begin{cases} \alpha = -x/2 \\ \tau = 2y \end{cases}$$

Recall that  $E$  is the ellipse  $x^2 + 4y^2 = r^2$ . Therefore  $jE$  is the ellipse  $4\alpha^2 + \tau^2 = r^2$ .

Let  $W$  denote the evolute of  $jE$ , in other words the envelope of normals which is the concave diamond with four cusps shown in Figure 8. Define the normal bundle  $M''$  of  $jE$  to be the subset of  $C \times jE$  given by

$$M'' = \{(c, e); c \in C, e \in jE, c \text{ lies on the normal at } e\}.$$

Now comes the surprise that justifies the construction.

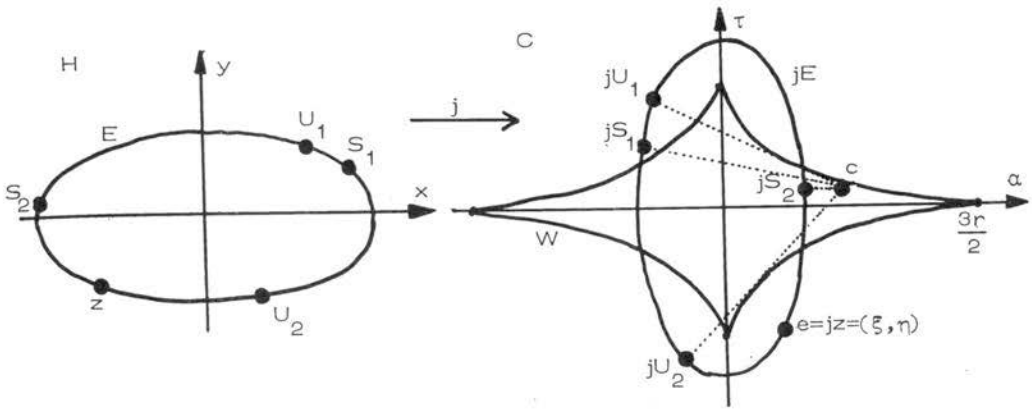


Figure 8.  $W$  is the evolute of  $jE$ . The harmonics of the stable and unstable equilibria corresponding to control point  $c$  are given by the inverse images  $S_1, S_2, U_1, U_2$  of the feet of the normals from  $c$  to  $jE$ .

Theorem 9.  $1 \times j: C \times E \rightarrow C \times jE$  maps  $M'$  diffeomorphically onto  $M''$ .

Proof. Let  $z = (x, y) \in H$ ,  $c = (\alpha, \tau) \in C$ . From the proof of Lemma 8, the total energy

$$\begin{aligned} V &= \frac{1}{4}(x^2 + 16y^2) + \alpha(x - 2\epsilon y) \\ &= \frac{1}{4}x^2 + 4y^2 + \alpha x - 4\tau y. \end{aligned}$$

The surface  $M' \subset C \times E$  is given by the stationary values of  $V$  with respect to  $x, y$ , subject to the constraint  $z \in E$ . Let  $e = jz \in C$ , and suppose  $e$  has coordinates  $e = (\xi, \eta)$ . Then

$$\begin{aligned} x &= -2\xi \\ y &= \eta/2. \\ V &= \xi^2 + \eta^2 - 2\alpha\xi - 2\tau\eta \\ &= (\xi - \alpha)^2 + (\eta - \tau)^2 - (\alpha^2 + \tau^2) \\ &= \delta^2 - (\alpha^2 + \tau^2) \end{aligned}$$

where  $\delta$  is the distance between the points  $c, e$ . The constraint becomes  $e \in jE$ . Therefore keeping  $c$  fixed and varying  $z$ ,

$$\begin{aligned}
 (c, z) \in M' &\iff V \text{ stationary, subject to } z \in E \\
 &\iff \delta \text{ stationary, subject to } e \in jE \\
 &\iff e \text{ is the foot of a normal from } c \\
 &\iff c \text{ lies on the normal at } e \\
 &\iff (c, e) \in M''
 \end{aligned}$$

Therefore  $1 \times j$  maps  $M'$  to  $M''$ , as required.

Problem. In the proof of Theorem 9 we used the second order approximation for  $V$ , and therefore the result is not proved over the whole of  $C$ , but only over an open subset  $U$  of  $C$ . However if  $r$  is small, then  $U$  contains the evolute  $W$ , which is the set we are really concerned with. It would be interesting to compute lower bounds for the size of  $U$  in terms of  $r$ . The subtlety of the problem is that Theorem 9 is strictly neither local or global, but semi-global.

Remark. The mysterious construction of  $j$  and the factor  $\frac{1}{2}$  in the definition of  $\tau$  were merely devices to identify the intrinsic Riemannian structure of the problem with that of the Euclidean plane.

The evolute  $W$ . We have reduced the geometry of  $M'$  to that of  $M''$ , which is well known. Topologically the normal bundle is a cylinder, showing that the equilibrium states are connected, and contain an essential cycle\*. Let  $c_e$  denote the centre of curvature of  $jE$  at  $e$ . Then the singular set of the projection  $\chi'' : M'' \rightarrow C$  is

$$\text{Sing } \chi'' = \{(c_e, e); e \in jE\}.$$

---

\* Hence a stiffened elastic panel can become locked in a global buckling mode, which cannot be localised and is difficult to push out. If you try to push it out then it will tend to slide around. The only way to get rid of it is to hold down the two second harmonics, and then press with sufficient force to call into play the third harmonic.

Therefore the bifurcation set

$$\text{Bif } \chi'' = \{c_e; e \in jE\} = \text{the evolute, } W.$$

Since the bifurcation sets of  $\chi, \chi' \chi''$  are all equal, we have achieved the desired result :

Corollary. Bif  $\chi = W$ .

This answers a question of Sewell [4].

The evolute can be written parametrically :

$$\left. \begin{aligned} \alpha &= \frac{3r}{2} \cos^3 \theta \\ \tau &= \frac{3r}{4} \sin^3 \theta, \quad 0 \leq \theta < 2\pi. \end{aligned} \right\}$$

The four cusp points are  $(\pm \frac{3r}{2}, 0), (0, \pm \frac{3r}{4})$ . In particular  $(\frac{3r}{2}, 0)$  is the cusp point of Theorem 8.

Geometric interpretation. Not only does the evolute give us the bifurcation set, in other words the loads and torques in  $C$  at which the catastrophic jumps take place, but the map  $j$  also enables us to identify the shapes of the strut, in other words the points in the harmonic plane  $H$  where the jumps begin and end.

Consider a point  $c$  in the interior of  $W$ , as in Figure 8. The four tangents from  $c$  to  $W$  are the same as the normals from  $c$  to  $jE$ . Let  $jS_1, jS_2, jU_1, jU_2$  be the feet of those normals, where  $S$  stands for stable (the distance from  $c$  to  $jE$  being a local minimum) and  $U$  stands for unstable (when it is a local maximum). Let  $S_1, S_2, U_1, U_2$  denote their inverse images under  $j$ . The latter points determine the shapes of the stable and unstable equilibria of the strut, corresponding to control  $c$ . For example Figure 5 illustrates the stable point  $S_1$ , with  $x, y > 0$ .

Now increase the load,  $\alpha$ . As  $c$  crosses  $W$  the points  $S_1$  and  $U_1$  coalesce, causing the stability of  $S_1$  to break down. Therefore the strut snaps into position  $S_2$ , with  $x < 0$ ,  $y > 0$ , as shown in Figure 9. Conversely

we can snap the strut up again by smoothly changing the sign of  $\alpha$  until  $c$  hits the left hand side of  $W$ , and then return the strut smoothly

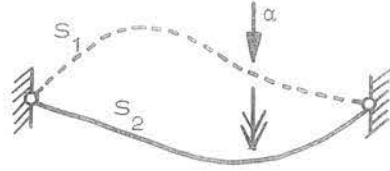


Figure 9. The snap  $S_1 \rightarrow S_2$ .

to its original position  $S_1$  by

increasing  $\alpha$  again. Alternatively we could return the strut to  $S_1$  along an entirely smooth path by making  $c$  encircle the top cusp of  $W$ .

Note that when  $c$  is at the top cusp the points  $S_1, U_1, S_2$  coalesce, confirming that it is an ordinary cusp catastrophe, with an unstable sheet in between two stables; similarly for the bottom cusp. Meanwhile when  $c$  is at the right hand cusp the points  $U_1, S_1, U_2$  coalesce, confirming that it is a dual cusp catastrophe, with a stable sheet in between two unstables, as we proved in Theorem 6 and Figure 6. Similarly with the left hand cusp. The global configuration is diffeomorphic to that of the catastrophe machine in [10].

Summarising, Figure 8 gives us a global comprehension of both the qualitative and the quantitative behaviour of the pinned Euler strut.

## REFERENCES

1. D. Chillingworth, The catastrophe of a bucking beam, *Dynamical Systems - Warwick 1974*, Springer Lecture Notes in Maths., 468, 86-91.
2. C.T.J. Dodson & M.M. Dodson, Simple non-linear systems and the cusp catastrophe, Lancaster & York Universities preprint, 1975.
3. L. Euler, Methodus inveniendi lineas curvas maximi minimive proprietate gaudentes (Appendix, De curvis elasticis), Marcum Michaelum Bousquet, Lausanne & Geneva, 1744.
4. M.J. Sewell, Some mechanical examples of catastrophe theory, *Bull. Inst. Math. and Appl.* (to appear).
5. J. Roorda, Stability of structures with small imperfections, *J. Engng. Mech. Div. Am. Soc. civ. Engrs.* 91, (1965) 87-106.
6. J.M.T. Thompson & G.W. Hunt, A general theory of elastic stability, Wiley, London, 1973.
7. J.M.T. Thompson & G.W. Hunt, Towards a unified bifurcation theory, *J. Appl. Math. & Physics* 26 (1975).
8. J.M.T. Thompson, Experiments in catastrophe, *Nature*, 254, 5499 (1975) 392-395.
9. D.J.A. Trotman & E.C. Zeeman, Classification of elementary catastrophes of codimension  $\leq 5$ , this volume.
10. E.C. Zeeman, A catastrophe machine, *Towards a theoretical biology*, 4 (Ed. C.H. Waddington), Edinburgh Univ. Press (1972), 276-282.
11. W.T. Koiter, On the stability of elastic equilibrium, *Dissertation*, Delft, Holland, 1945.
12. M.J. Sewell, The static perturbation technique in buckling problems, *J. Mech. Phys. Solids*, 13, 247 (1965).